

Loss of host-derived osteopontin creates a glioblastoma-promoting microenvironment

Frank Szulzewsky, Nina Schwendinger, Dilansu Güneykaya, Patrick J Cimino, Dolores Hambardzumyan, Michael Synowitz, Eric C Holland, Helmut Kettenmann

Supplementary data

Suppl. Table S1: List of antibodies used for flow cytometry

Suppl. Table S2: List of primers used for qRT-PCRs

Suppl. Table S3: List of antibodies used for immunofluorescence staining

Suppl. Figure S1: TCGA gene expression data shows that *OPN/SPP1* expression in human GBM whole tumor samples strongly correlates with the expression of myeloid cell markers *CD68*, *PTPRC/CD45*, *ITGAM/CD11b*, and *HAVCR2*, but not with general tumor cell markers *GFAP*, *OLIG2*, *SOX2*, *EGFR*, *CDKN2A*, *CDK4*, *TP53*, *GLI1*. Pearson correlation was used to calculate correlation coefficients.

Suppl. Figure S2: A and B: Isoform specific primers were used to determine the expression of the different *OPN/SPP1* transcript variants in human non-tumor brain $CD11b^+$ samples, $CD11b^+$, and $CD11b^-$ GBM cell fractions. Δ ct values relative to *ACTB* expression (A) and fold changes relative to non-tumor brain $CD11b^+$ samples (B) are shown. Error bars represent SD. C and D: One-Way ANOVA multiple comparison statistics are shown for Graph A (C) and Graph B (D). E and F: The expression of *AIF1/Iba1* (E) and *GFAP* (F) was measured in $CD11b^+$ (n = 8) and $CD11b^-$ (n = 4) fractions to assess purity of the samples. Error bars represent SEM.

Suppl. Figure S3: Representative images from sections of three human GBM samples stained for Iba1 and OPN. Left panel: 10x objective, bar represents 100 μ m Right panel: 40x objective, bar represents 50 μ m

Suppl. Figure S4: Images taken from human GBM sections stained for OPN and Iba1 showing Osteopontin staining that does not co-localize with Iba1 staining. 10x objective, bar represents 100 μ m

Suppl. Figure S5: A: Graph showing the percent of OPN^+ cells in $CD11b^+$ and $CD11b^-$ fractions from mouse naïve brains (n=2) and GL261 tumors (n=4). B: One-Way ANOVA multiple comparison statistics are shown for Graph A C: Plots depicting the strategy for isolation of microglia and macrophages/monocytes from naïve brains, naïve spleens, and GL261 glioma-bearing brains using *Cx3cr1^{GFP/wt} Ccr2^{RFP/wt}* mice. D: Percentages of GFP^+/RFP^- microglia and GFP^{low}/RFP^+ macrophages/monocytes in cell isolates from GL261 tumor core and border regions. Statistics were calculated using One-Way-ANOVA. E: Isoform specific primers were used to determine the expression of the different *OPN/SPP1* transcript variants in the GFP^+/RFP^- , GFP^{low}/RFP^+ , and GFP^-/RFP^- cell fractions of GL261 tumors that were implanted into *Cx3cr1^{GFP/wt} Ccr2^{RFP/wt}* mice. F: One-Way ANOVA multiple comparison statistics are shown for Graph E

Suppl. Figure S6: A: Western Blot of three neonatal microglia lysates and three GL261 cell lysates stained for mouse OPN and beta-Actin. B and C: OPN staining in Iba1⁺ cells co-localizes with the Golgi marker GRASP65 in human GBM samples (B) and mouse GL261 tumors (C). D and E: Original z stack images that were used for the 3D reconstructions in Figure 2 D and E. F and G: 3D reconstructions and original z stack images of co-stainings of human (F) and mouse (G) tumors for Iba1, OPN, and LAMP1. Bars represents 25 μ m (B and C) and 3 μ m (D-G).

Suppl. Figure S7: Graph showing the average weight progression of GL261 implanted OPN^{-/-} and wild type mice (n = 10 for each group). P value was calculated by linear regression. Error bars represent SD.

Suppl. Figure S8: Representative images of GL261 tumors in wild type and OPN^{-/-} mice. A: Sections stained with CD31 and GFAP. GFAP staining is restricted to the tumor border areas but absent in tumor core. Upper panels: 10x objective. Middle and lower panels: 20x objective. Bars represent 100 μ m. B: Sections stained with CD31 and AQP4. AQP4 staining is restricted to the tumor border areas but absent in tumor core. Upper panels: 10x objective. Middle and lower panels: 20x objective. Bars represent 100 μ m.

Suppl. Figure S9: Layout showing the gating strategy used to analyse the immune cell compartment in naïve brains and tumor-bearing OPN^{-/-} and wild type mice

Suppl. Table S1

CD45	eFlour450	eBioscience
CD11b	Alexa700	eBioscience
CD3	APC	eBioscience
CD4	FITC	eBioscience
CD8	PE	eBioscience
CD196	brillant violet 421	Biolegend
OPN	PE	RD Systems IC808P

Supplementary Table S2

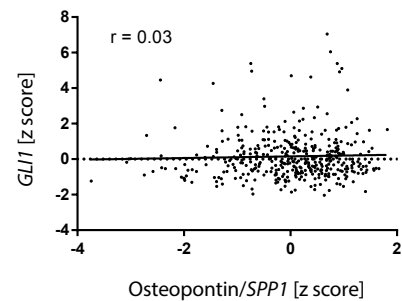
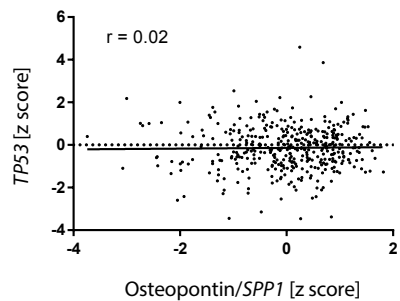
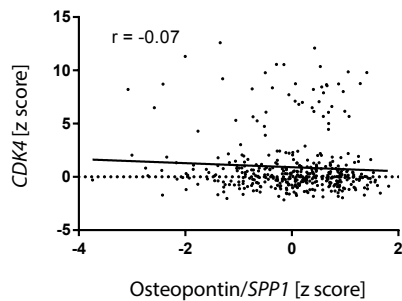
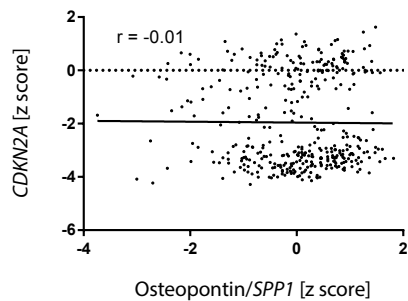
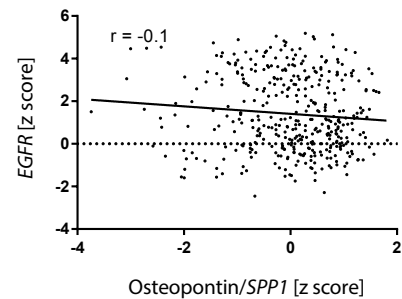
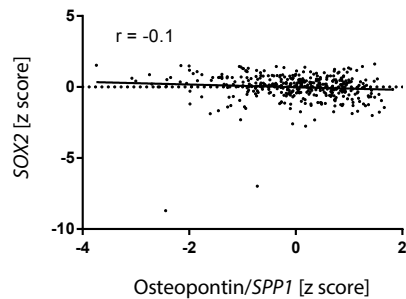
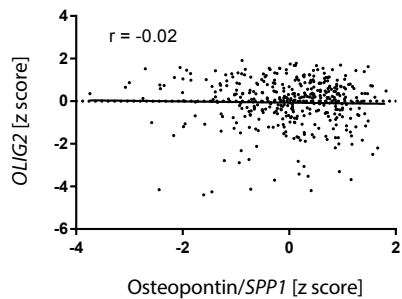
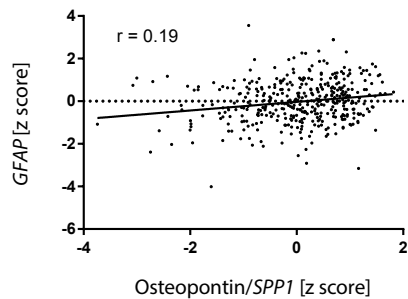
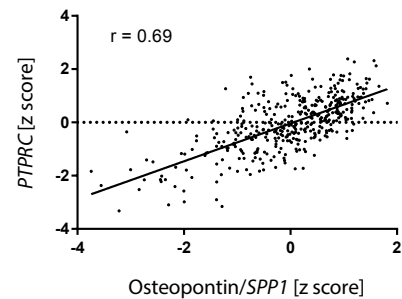
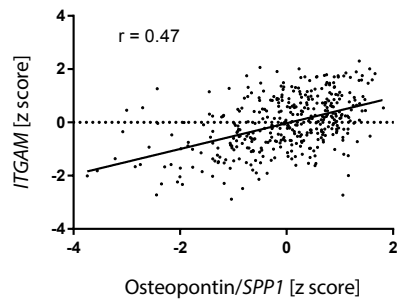
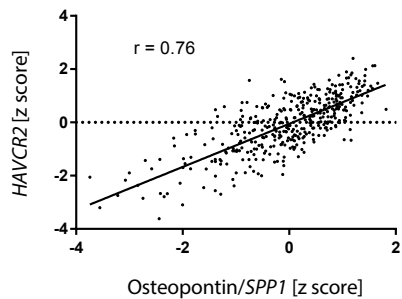
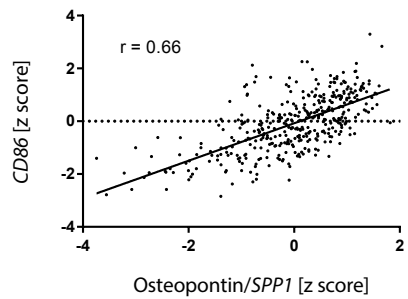
human SPP1 Fwd	GCCGAGGTGATAGTGTGGTT
human SPP1 Rev	AACGGGGATGGCCTTGTATG
human Actb Fwd	GAGCTACGAGCTGCCTGAC
human Actb Rev	GACTCCATGCCAGGAAGG
mouse Actb Fwd	CGTGGGCCGCCCTAGGCACCA
mouse Actb Rev	CTTAGGGTTCAGGGGGGC
mouse Arg1 Fwd	GGCAGAGGTCCAGAAGAATGG
mouse Arg1 Rev	AGCATCCACCCAAATGACACA
mouse Cd86 Fwd	ACAACCAGACTCCTGTAGACG
mouse Cd86 Rev	TGTAATGGGCACGGCAGAT
mouse Cd163 Fwd	ACTCTAAAACCTGGGGCAACAAA
mouse Cd163 Rev	TGGGATTTCCTCCAACCA
mouse Cd206 Fwd	GACTGTGTAGTTGTGATTGGTGG
mouse Cd206 Rev	AAGCCATCTTTGGAGTAGTGGT
mouse Ifng Fwd	TTACTACCTTCTCAGCAACAGCAA
mouse Ifng Rev	GCGACTCCTTTCCGCTTCC
mouse Il1b Fwd	TGGTGTGTGACGTTCCATT
mouse Il1b Rev	TGTCCATTGAGGTGGAGAGC
mouse Il1r2 Fwd	AGGCAAGAAGCAGCAAGGTA
mouse Il1r2 Rev	CTGTTGGAGTGGTGAAAGCAG
mouse Il1rn Fwd	CAGAAAGGGCGGGAGATTTT
mouse Il1rn Rev	GGTTCATGGTGGAACAACACT
mouse Il6 Fwd	ACAAAGAAATGATGGATGCTACCAA
mouse Il6 Rev	GTACTIONCAGAAGACCAGAGGAAA
mouse Il10 Fwd	CCAAGCCTTATCGGAAATGAT
mouse Il10 Rev	ATCCTGAGGGTCTTCAGCTTC
mouse Il27 Fwd	CTGTTGCTGCTACCCTTGCTT
mouse Il27 Rev	CACTCCTGGCAATCGAGATTC
mouse Irf7 Fwd	GCCCAAGGAGAAGACCCTGA
mouse Irf7 Rev	AGACAAGCACAAAGCCGAGAC
mouse Mmp9 Fwd	CATTGCGGTGGATAAGGAGT
mouse Mmp9 Rev	ACCTGGTTCACCTCATGGTC
mouse Mmp14 Fwd	GTGCCCTATGCCTACATCCG
mouse Mmp14 Rev	CAGCCACCAAGAAGATGTCA
mouse Nos2 Fwd	GGACGAGACGGATAGGCAGA
mouse Nos2 Rev	CGTGGGGTTGTTGCTGAACT
mouse Ptgs2 Fwd	AGCACTTCACCCATCAGTTTTT
mouse Ptgs2 Rev	ATACACCTCTCCACCAATGACC
mouse Spp1 Fwd	AGCAAGAAACTCTTCCAAGCAA
mouse Spp1 Rev	GTGAGATTGCTCAGATTCATCCG
mouse Stat3 Fwd	CAGTTCTCGTCCACCACCAAG
mouse Stat3 Rev	GACACCTGAGTAGTTCACACC
mouse TNFa Fwd	AGGAGGAGTCTGCGAAGAAGA
mouse TNFa Rev	GGCAGTGGACCATCTAACTCG
mouse Vegfa Fwd	GCACATAGGAGAGATGAGCTT
mouse Vegfa Rev	TCTGGCTTTGTTCTGTCTTTCT
human SPP1tv1-2 Fwd	CCTCCTAGGCATCACCTGTGCCAT
human SPP1tv1 Rev	CATTGGTTTCTTCAGAGGACACAG

human SPP1tv2 Rev	TTGGAAGGGTCTGTGGGGCTAGG
human SPP1tv3-5 Fwd	GAATTGCAGTGATTTGCTTTTGC
human SPP1tv3 Rev	AGGACACAGCATTCTGCTTTTC
human SPP1tv4 Rev	GGAAGGGTCTGCTTTTCCTCA
human SPP1tv5 Rev	AGGTACATCTTTAGTGCTGCTTTTC
mouse Spp1tv1-2 Fwd	CCTGGCTGAATTCTGAGGGACTAA
mouse Spp1tv1-2 Rev	CAATGCCAAACAGGCAAAAGCA
mouse Spp1tv3-4 Fwd	CAGCCAAGGACTAACTACGACC
mouse Spp1tv3-4 Rev	TTCTGTGGCGCAAGGAGATTC
mouse Spp1tv5 Fwd	ACTTGGTGGTGATCTAGTGGTG
mouse Spp1tv5 Rev	ACTGCCAATCTCATGGTCGTA
human AIF1 Fwd	CGAATGCTGGAGAACTTGGA
human AIF1 Rev	GAAAGTCAGGGTAGCTGAACG
human GFAP Fwd	CGCACGCAGTATGAGGCAA
human GFAP Rev	GACTCCAGGTCGCAGGTCAA

Suppl. Table S3

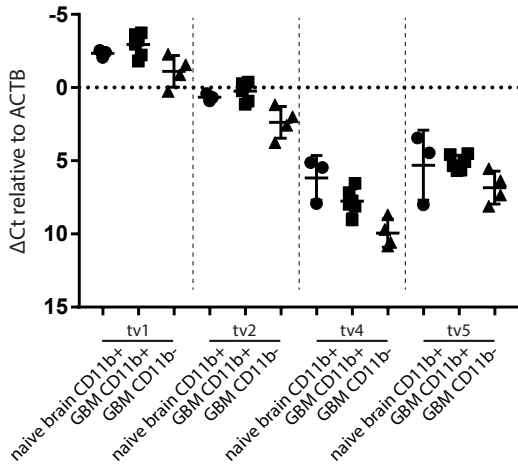
AQP4	A5971	1:150	Sigma
CD31	DIA-310	1:100	Histobiotech
GFAP	Z0334	1:8000	Dako
GRASP65	PA3-910	1:100	Thermo Scientific
Iba1	ab124800	1:200	abcam
Iba1	019-19741	1:500	Wako
Ki67	VP-RM04	1:200	Vector
PDGFRbeta	3169	1:300	Cell Signaling
human OPN	AF1433	1:2000	R&D Systems
mouse OPN	AF808	1:1000	R&D Systems
human LAMP1	9091	1:200	Cell Signaling
mouse LAMP1	MAB4320	1:100	R&D Systems

Suppl. Figure S1

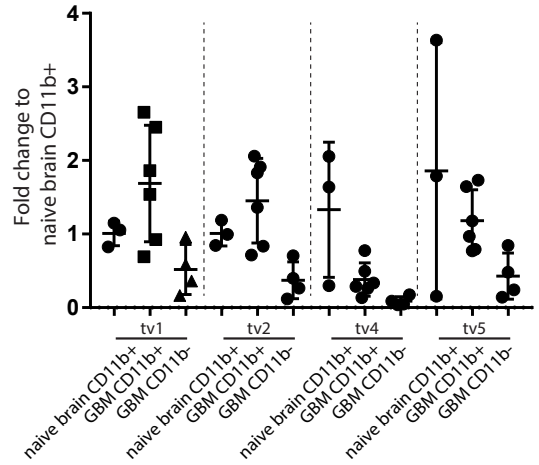


Suppl. Figure S2

A Expression of human *SPP1*/Osteopontin transcript variants (tv)



B Expression of human *SPP1*/Osteopontin transcript variants (tv)



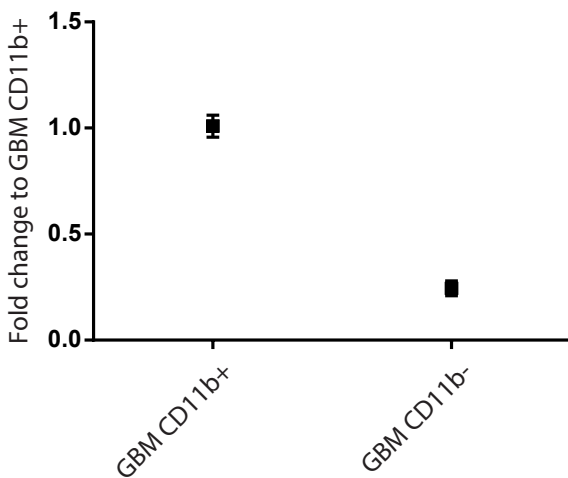
C ANOVA multiple comparison statistics for ΔC_t values (Graph A)

Tukey's multiple comparisons test	Mean Diff.	95.00% CI of diff.	Adjusted P Value
naive brain CD11b+ tv1 vs. GBM CD11b+ tv1	0.596	-1.86 to 3.052	0.9993
naive brain CD11b+ tv1 vs. GBM CD11b- tv1	-1.227	-3.881 to 1.426	0.8975
naive brain CD11b+ tv1 vs. naive brain CD11b+	-3.003	-5.84 to -0.1669	0.0298
naive brain CD11b+ tv1 vs. naive brain CD11b+	-8.51	-11.35 to -5.674	<0.0001
naive brain CD11b+ tv1 vs. naive brain CD11b+	-7.64	-10.48 to -4.804	<0.0001
GBM CD11b+ tv1 vs. GBM CD11b- tv1	-1.823	-4.066 to 0.419	0.2104
GBM CD11b+ tv1 vs. GBM CD11b+ tv2	-3.175	-5.18 to -1.169	0.0001
GBM CD11b+ tv1 vs. GBM CD11b+ tv4	-10.7	-12.71 to -8.695	<0.0001
GBM CD11b+ tv1 vs. GBM CD11b+ tv5	-8.07	-10.08 to -6.065	<0.0001
GBM CD11b- tv1 vs. GBM CD11b- tv2	-3.486	-5.942 to -1.03	0.0008
GBM CD11b- tv1 vs. GBM CD11b- tv4	-11.06	-13.51 to -8.602	<0.0001
GBM CD11b- tv1 vs. GBM CD11b- tv5	-7.951	-10.41 to -5.495	<0.0001
naive brain CD11b+ tv2 vs. GBM CD11b+ tv2	0.4248	-2.032 to 2.881	>0.9999
naive brain CD11b+ tv2 vs. GBM CD11b- tv2	-1.71	-4.363 to 0.9432	0.5358
naive brain CD11b+ tv2 vs. naive brain CD11b+	-5.507	-8.343 to -2.67	<0.0001
naive brain CD11b+ tv2 vs. naive brain CD11b+	-4.637	-7.473 to -1.8	<0.0001
GBM CD11b+ tv2 vs. GBM CD11b- tv2	-2.135	-4.377 to 0.1075	0.0747
GBM CD11b+ tv2 vs. GBM CD11b+ tv4	-7.527	-9.532 to -5.521	<0.0001
GBM CD11b+ tv2 vs. GBM CD11b+ tv5	-4.896	-6.901 to -2.89	<0.0001
GBM CD11b- tv2 vs. GBM CD11b- tv4	-7.572	-10.03 to -5.116	<0.0001
GBM CD11b- tv2 vs. GBM CD11b- tv5	-4.465	-6.921 to -2.009	<0.0001
naive brain CD11b+ tv4 vs. GBM CD11b+ tv4	-1.595	-4.051 to 0.8614	0.5248
naive brain CD11b+ tv4 vs. GBM CD11b- tv4	-3.776	-6.429 to -1.122	0.0008
naive brain CD11b+ tv4 vs. naive brain CD11b+ tv5	0.87	-1.966 to 3.706	0.9947
GBM CD11b+ tv4 vs. GBM CD11b- tv4	-2.181	-4.423 to 0.06173	0.0631
GBM CD11b+ tv4 vs. GBM CD11b+ tv5	2.631	0.625 to 4.636	0.0026
GBM CD11b- tv4 vs. GBM CD11b- tv5	3.107	0.6508 to 5.564	0.0041
naive brain CD11b+ tv5 vs. GBM CD11b+ tv5	0.1657	-2.291 to 2.622	>0.9999
naive brain CD11b+ tv5 vs. GBM CD11b- tv5	-1.538	-4.192 to 1.115	0.6839
GBM CD11b+ tv5 vs. GBM CD11b- tv5	-1.704	-3.946 to 0.5383	0.295

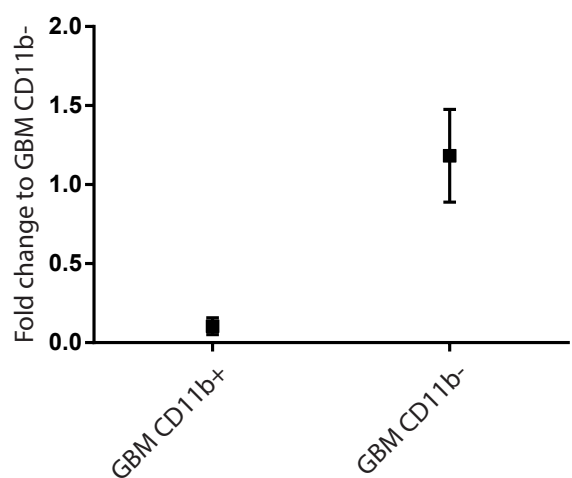
D ANOVA multiple comparison statistics for Fold change values (Graph B)

Tukey's multiple comparisons test	Mean Diff.	95.00% CI of diff.	Adjusted P Value
naive brain CD11b+ tv1 vs. GBM CD11b+ tv1	-0.6774	-2.161 to 0.8065	0.9052
naive brain CD11b+ tv1 vs. GBM CD11b- tv1	0.4927	-1.11 to 2.095	0.9946
naive brain CD11b+ tv1 vs. naive brain CD11b+ tv2	-8.3E-05	-1.714 to 1.713	>0.9999
naive brain CD11b+ tv1 vs. naive brain CD11b+ tv4	-0.3208	-2.034 to 1.393	>0.9999
naive brain CD11b+ tv1 vs. naive brain CD11b+ tv5	-0.8497	-2.563 to 0.8638	0.8487
GBM CD11b+ tv1 vs. GBM CD11b- tv1	1.17	-0.1845 to 2.525	0.1477
GBM CD11b+ tv1 vs. GBM CD11b+ tv2	0.2349	-0.9767 to 1.446	>0.9999
GBM CD11b+ tv1 vs. GBM CD11b+ tv4	1.305	0.09362 to 2.517	0.0252
GBM CD11b+ tv1 vs. GBM CD11b+ tv5	0.5058	-0.7058 to 1.717	0.9459
GBM CD11b- tv1 vs. GBM CD11b- tv2	0.1453	-1.339 to 1.629	>0.9999
GBM CD11b- tv1 vs. GBM CD11b- tv4	0.4299	-1.054 to 1.914	0.9967
GBM CD11b- tv1 vs. GBM CD11b- tv5	0.08903	-1.395 to 1.573	>0.9999
naive brain CD11b+ tv2 vs. GBM CD11b+ tv2	-0.4425	-1.926 to 1.041	0.9958
naive brain CD11b+ tv2 vs. GBM CD11b- tv2	0.638	-0.9648 to 2.241	0.9608
naive brain CD11b+ tv2 vs. naive brain CD11b+ tv4	-0.3207	-2.034 to 1.393	>0.9999
naive brain CD11b+ tv2 vs. naive brain CD11b+ tv5	-0.8496	-2.563 to 0.8639	0.8488
GBM CD11b+ tv2 vs. GBM CD11b- tv2	1.081	-0.2741 to 2.435	0.2331
GBM CD11b+ tv2 vs. GBM CD11b+ tv4	1.07	-0.1413 to 2.282	0.1278
GBM CD11b+ tv2 vs. GBM CD11b+ tv5	0.271	-0.9406 to 1.483	0.9997
GBM CD11b- tv2 vs. GBM CD11b- tv4	0.2846	-1.199 to 1.768	>0.9999
GBM CD11b- tv2 vs. GBM CD11b- tv5	-0.05628	-1.54 to 1.428	>0.9999
naive brain CD11b+ tv4 vs. GBM CD11b+ tv4	0.9485	-0.5354 to 2.432	0.548
naive brain CD11b+ tv4 vs. GBM CD11b- tv4	1.243	-0.3595 to 2.846	0.268
naive brain CD11b+ tv4 vs. naive brain CD11b+ tv5	-0.5289	-2.242 to 1.185	0.9944
GBM CD11b+ tv4 vs. GBM CD11b- tv4	0.2947	-1.06 to 1.649	0.9998
GBM CD11b+ tv4 vs. GBM CD11b+ tv5	-0.7994	-2.011 to 0.4122	0.5009
GBM CD11b- tv4 vs. GBM CD11b- tv5	-0.3408	-1.825 to 1.143	0.9996
naive brain CD11b+ tv5 vs. GBM CD11b+ tv5	0.678	-0.8059 to 2.162	0.9047
naive brain CD11b+ tv5 vs. GBM CD11b- tv5	1.431	-0.1715 to 3.034	0.1189
GBM CD11b+ tv5 vs. GBM CD11b- tv5	0.7533	-0.6013 to 2.108	0.7353

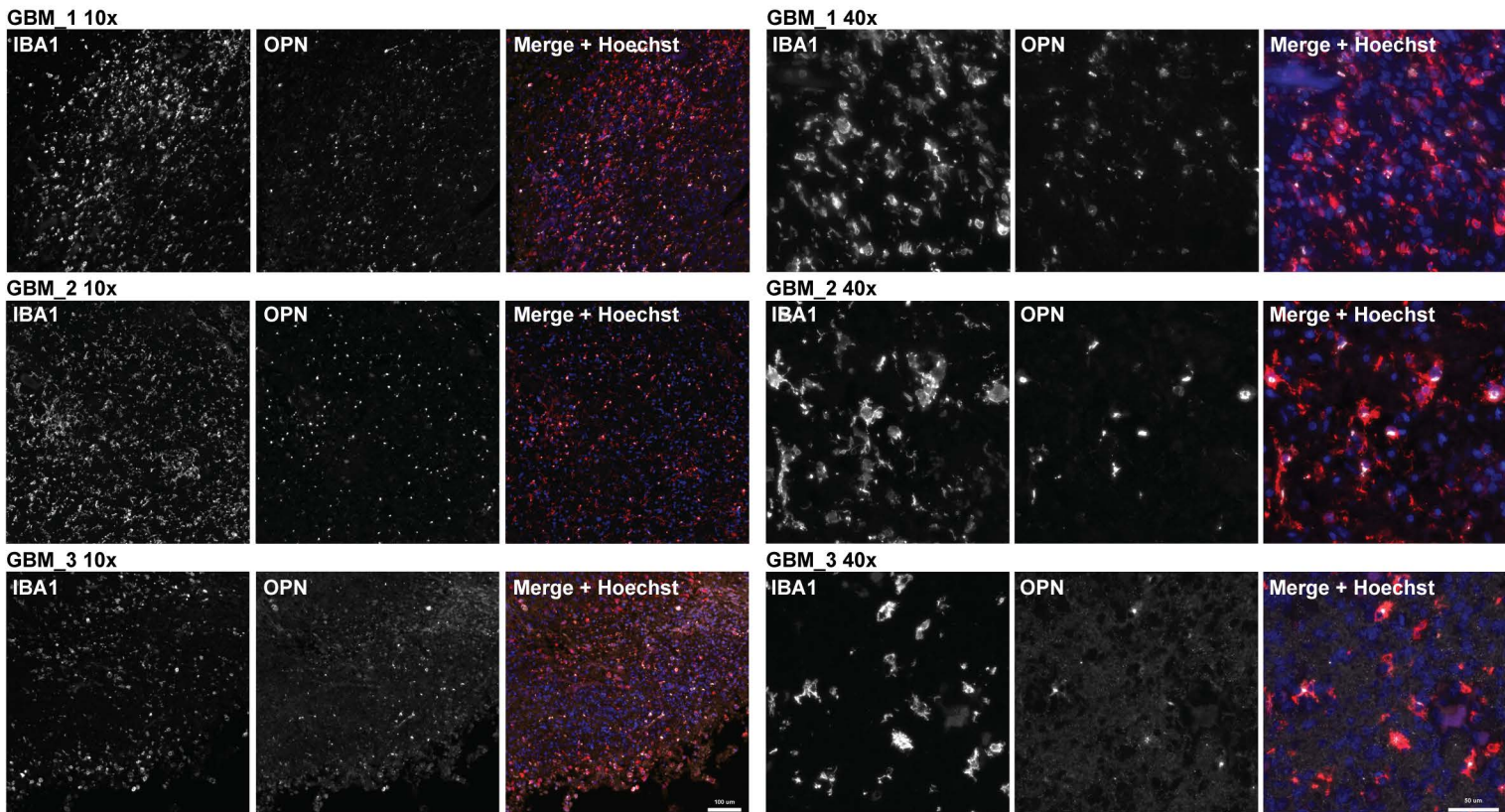
E Expression of *AIF1*/Iba1 in human GBM fractions



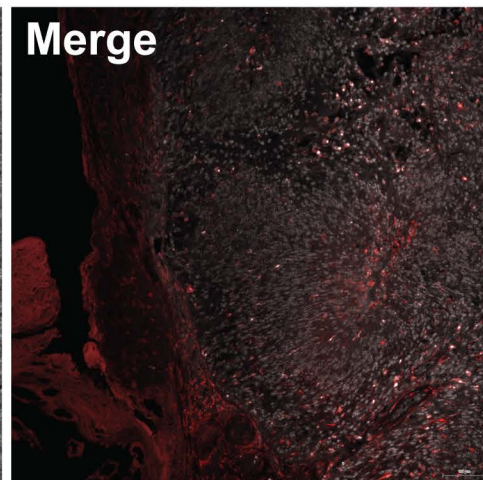
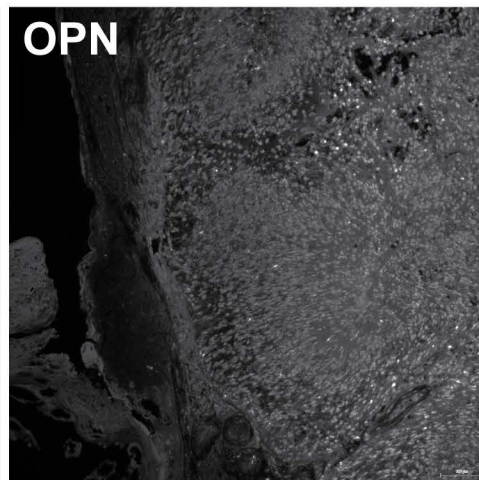
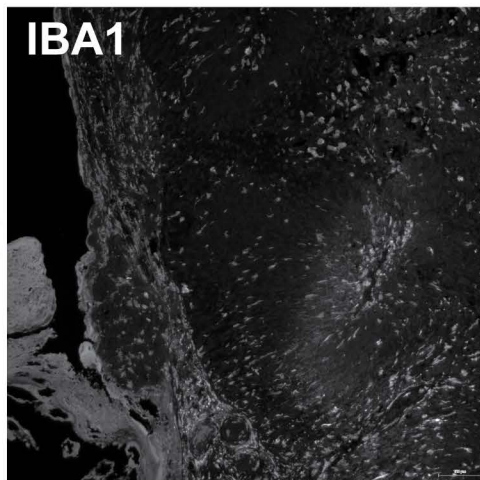
F Expression of *GFAP* in human GBM fractions



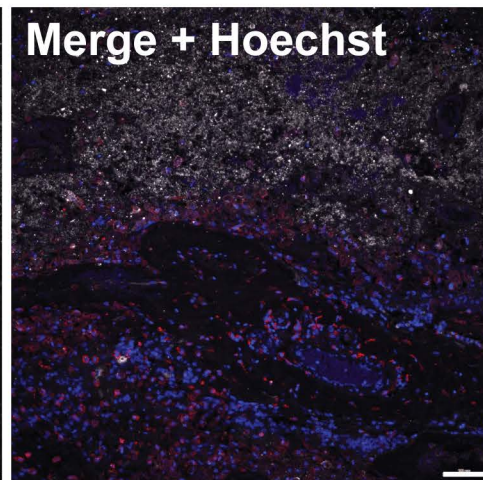
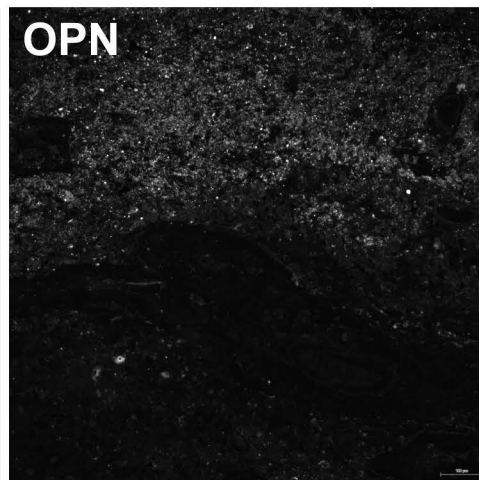
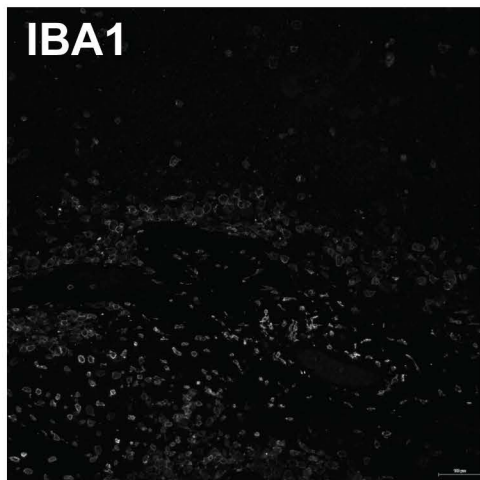
Suppl. Figure S3



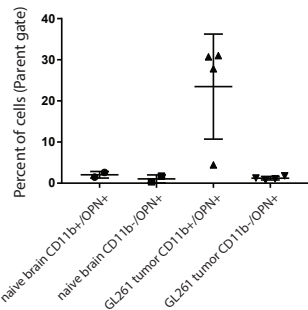
Area 1



Area 2

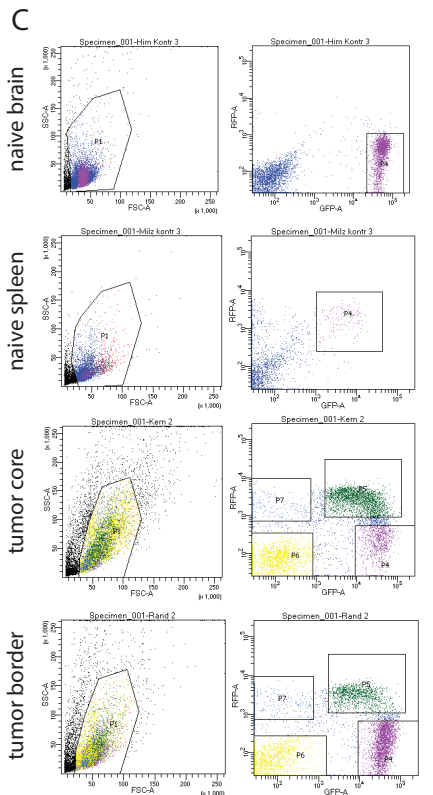


A Osteopontin/*Spp1*-expressing cells in naive brain and GL261 tumors by flow cytometry

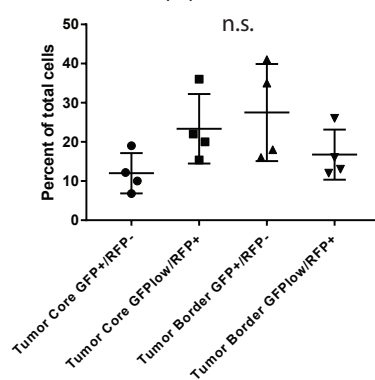


B ANOVA multiple comparison statistics for Graph A

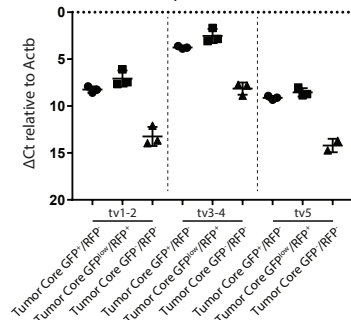
Tukey's multiple comparisons test	Mean Diff.	95.00% CI of diff.	Adjusted P Value
CTR CD11b+ OPN+ vs. CTR CD11b- OPN+	1.015	-24.09 to 26.12	0.9992
CTR CD11b+ OPN+ vs. Tumor CD11b+ OPN+	-21.44	-43.18 to 0.3029	0.0532
CTR CD11b+ OPN+ vs. Tumor CD11b- OPN+	0.84	-20.9 to 22.58	0.9993
CTR CD11b- OPN+ vs. Tumor CD11b+ OPN+	-22.45	-44.19 to -0.7121	0.0432
CTR CD11b- OPN+ vs. Tumor CD11b- OPN+	-0.175	-21.92 to 21.57	>0.9999
Tumor CD11b+ OPN+ vs. Tumor CD11b- OPN+	22.28	4.527 to 40.03	0.0162



D Immune cell populations in GL261 tumors



E Expression of mouse *Spp1*/Osteopontin transcript variants (tv)

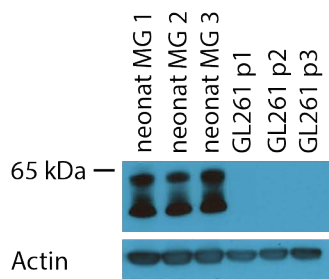


F ANOVA multiple comparison statistics for ΔC_t values mouse SPP1/Osteopontin transcript variants

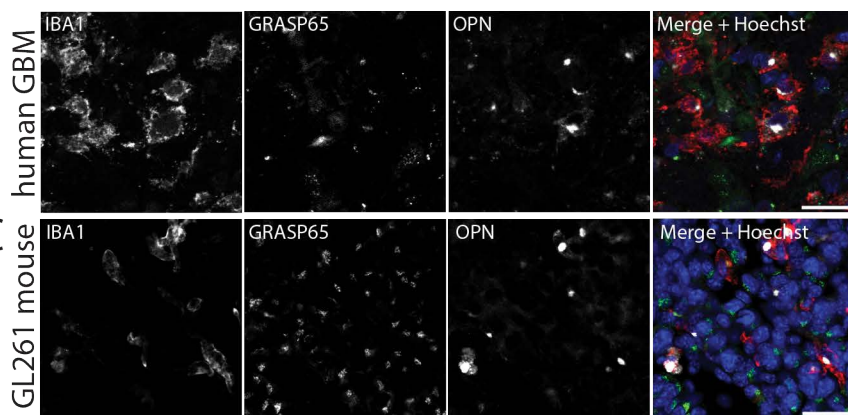
Tukey's multiple comparisons test	Mean Diff.	95.00% CI of diff.	Adjusted P Value
Tumor Core GFP+/RFP- tv1-2 vs. Tumor Core GFPloW/RFP+ tv1-2	1.173	-0.6418 to 2.988	0.4027
Tumor Core GFP+/RFP- tv1-2 vs. Tumor Core GFP-/RFP- tv1-2	-4.997	-6.812 to -3.182	<0.0001
Tumor Core GFP+/RFP- tv1-2 vs. Tumor Core GFP+/RFP- tv3-4	4.49	2.675 to 6.305	<0.0001
Tumor Core GFP+/RFP- tv1-2 vs. Tumor Core GFP+/RFP- tv5	-0.877	-2.692 to 0.9381	0.7362
Tumor Core GFPloW/RFP+ tv1-2 vs. Tumor Core GFP-/RFP- tv1-2	-6.17	-7.985 to -4.355	<0.0001
Tumor Core GFPloW/RFP+ tv1-2 vs. Tumor Core GFPloW/RFP+ tv3-4	4.532	2.723 to 6.353	<0.0001
Tumor Core GFPloW/RFP+ tv1-2 vs. Tumor Core GFPloW/RFP+ tv5	-1.467	-3.282 to 0.3478	0.1699
Tumor Core GFP-/RFP- tv1-2 vs. Tumor Core GFP-/RFP- tv3-4	5.099	3.284 to 6.914	<0.0001
Tumor Core GFP-/RFP- tv1-2 vs. Tumor Core GFP-/RFP- tv5	-0.9953	-2.999 to 1.00	0.747
Tumor Core GFP+/RFP- tv3-4 vs. Tumor Core GFPloW/RFP+ tv3-4	1.221	-0.5941 to 3.036	0.3555
Tumor Core GFP+/RFP- tv3-4 vs. Tumor Core GFP-/RFP- tv3-4	-4.388	-6.203 to -2.573	<0.0001
Tumor Core GFP+/RFP- tv3-4 vs. Tumor Core GFP+/RFP- tv5	-5.367	-7.182 to -3.552	<0.0001
Tumor Core GFPloW/RFP+ tv3-4 vs. Tumor Core GFP-/RFP- tv3-4	-6.609	-7.424 to -3.794	<0.0001
Tumor Core GFPloW/RFP+ tv3-4 vs. Tumor Core GFPloW/RFP+ tv5	-6.005	-7.82 to -4.19	<0.0001
Tumor Core GFP-/RFP- tv3-4 vs. Tumor Core GFP-/RFP- tv5	-6.069	-8.095 to -4.039	<0.0001
Tumor Core GFP+/RFP- tv5 vs. Tumor Core GFPloW/RFP+ tv5	0.553	-1.232 to 2.398	0.9602
Tumor Core GFP+/RFP- tv5 vs. Tumor Core GFP-/RFP- tv5	-5.089	-7.118 to -3.06	<0.0001
Tumor Core GFPloW/RFP+ tv5 vs. Tumor Core GFP-/RFP- tv5	-5.672	-7.701 to -3.643	<0.0001

Suppl. Figure S6

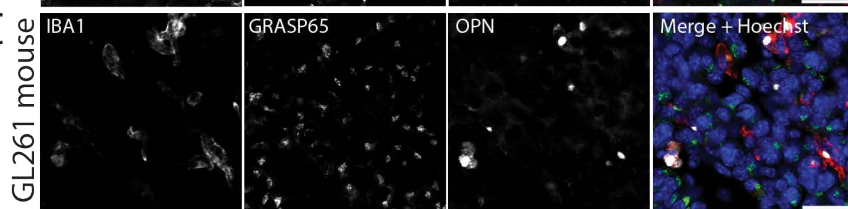
A



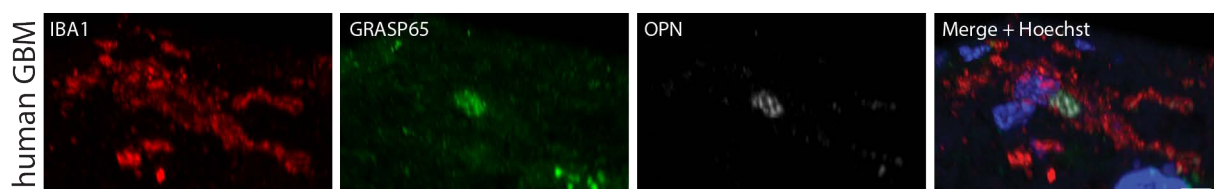
B



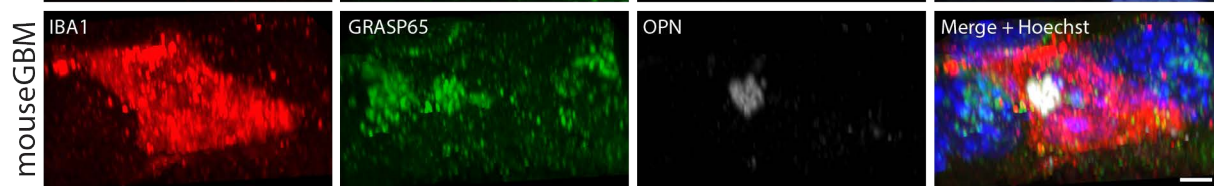
C



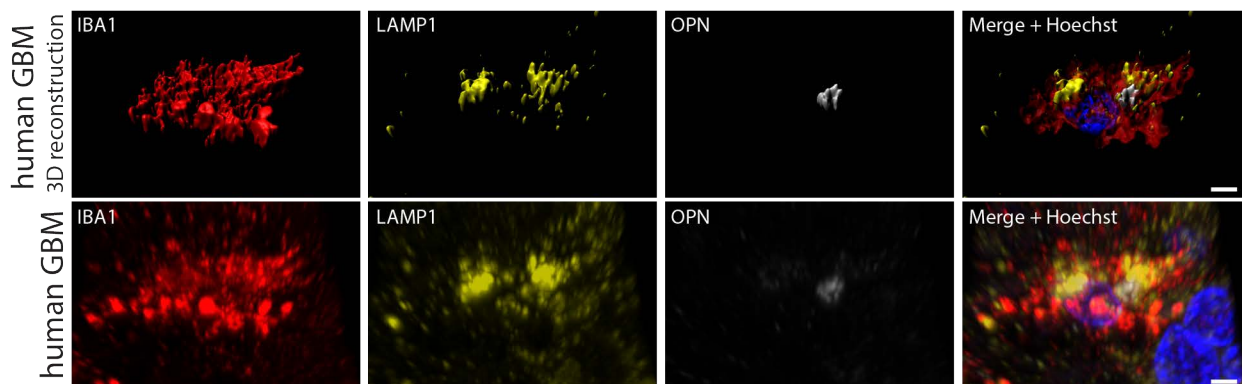
D



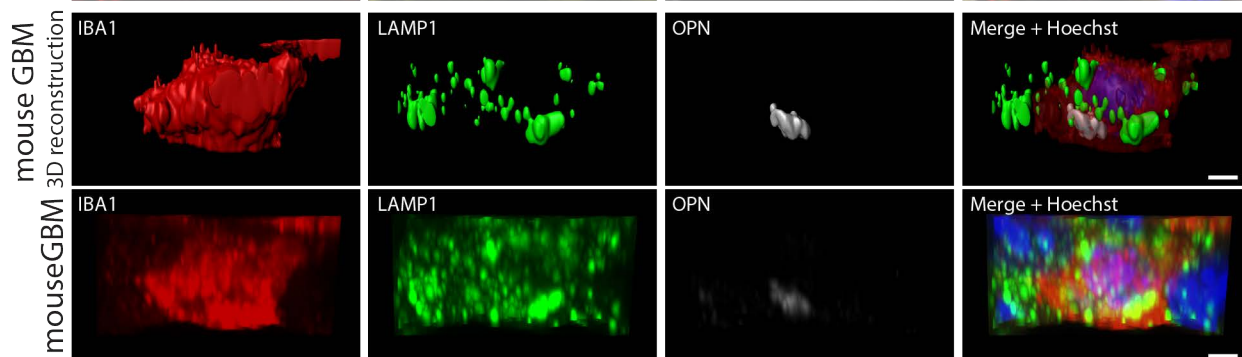
E



F

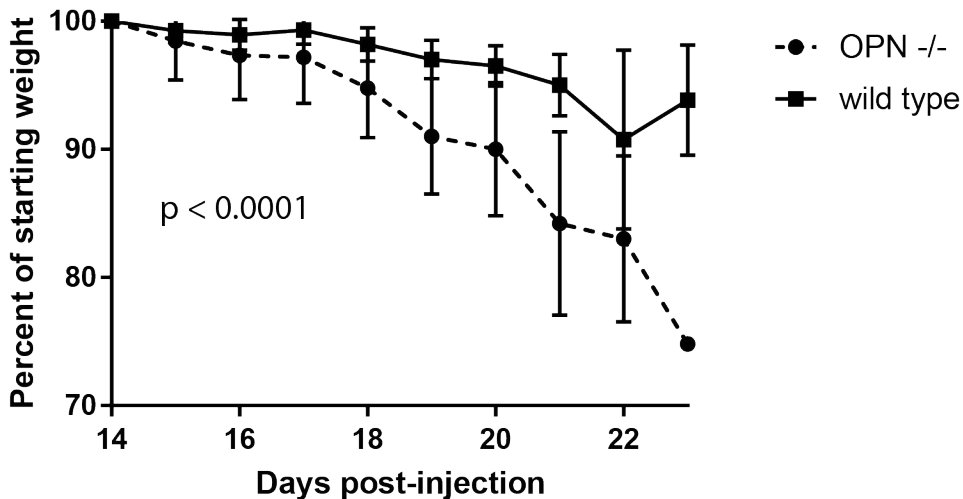


G



Suppl. Figure S7

Weight progression

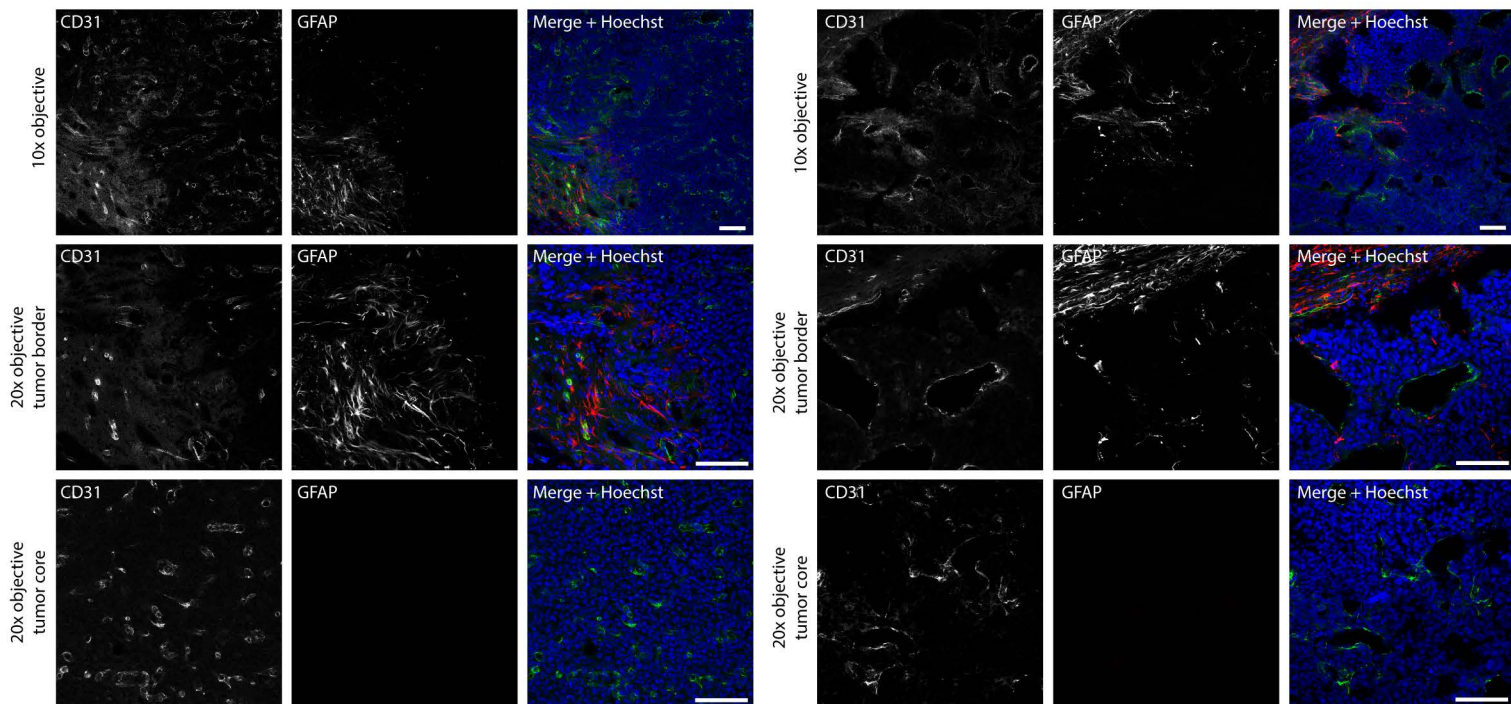


Suppl. Figure S8

A

GL261 tumor in wild type mouse

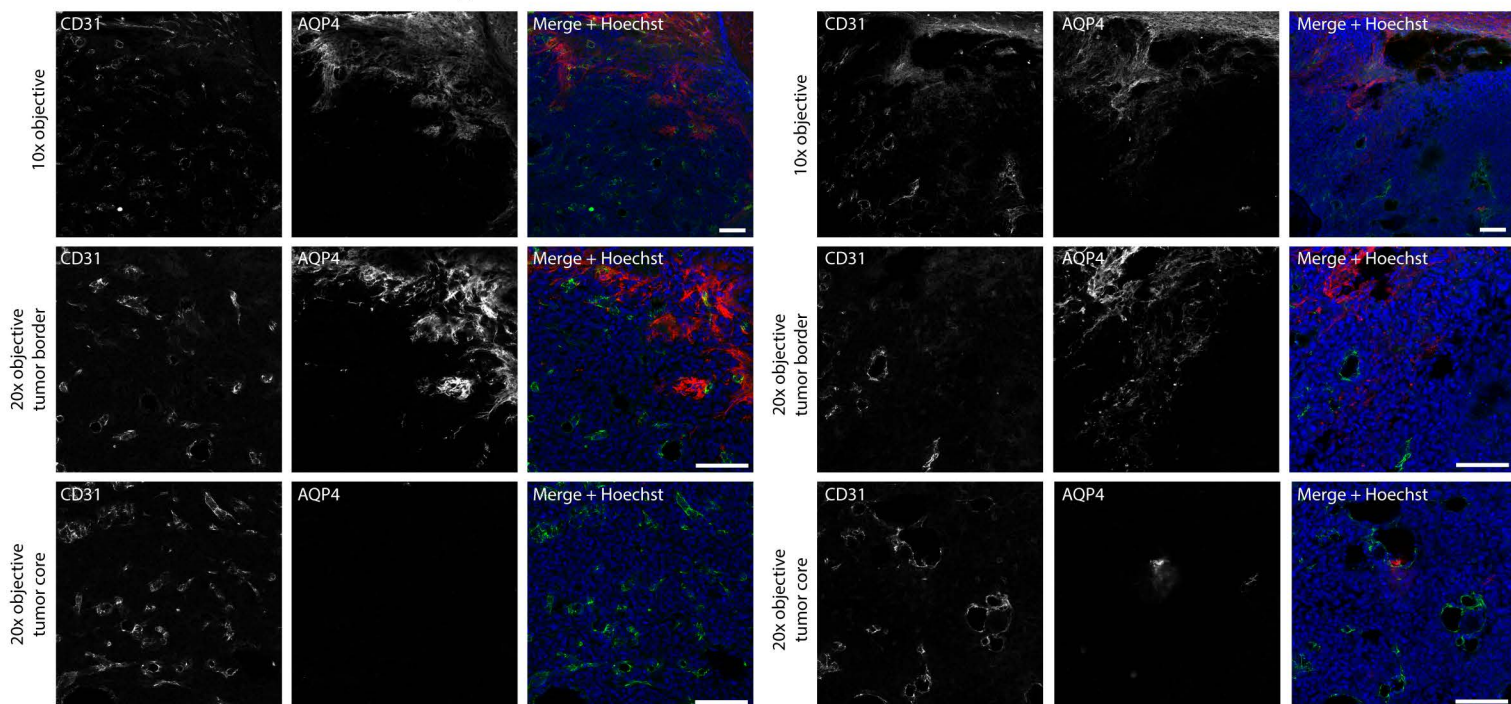
GL261 tumor in OPN^{-/-} mouse



B

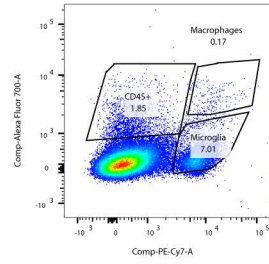
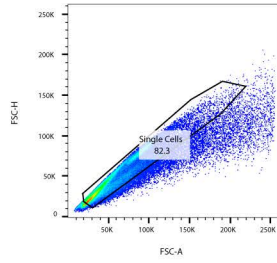
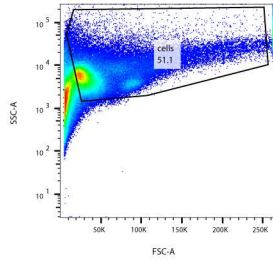
GL261 tumor in wild type mouse

GL261 tumor in OPN^{-/-} mouse

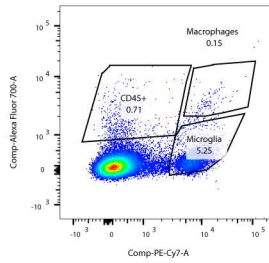
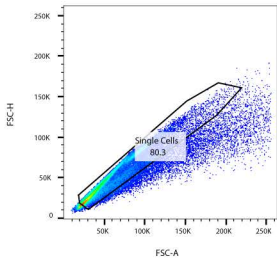
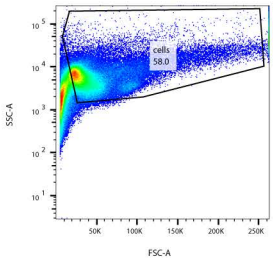


Suppl. Figure S9

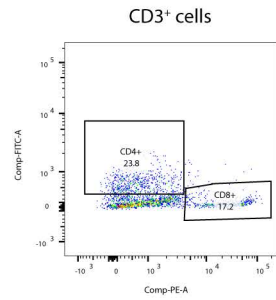
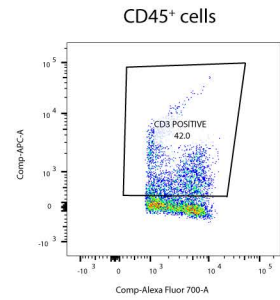
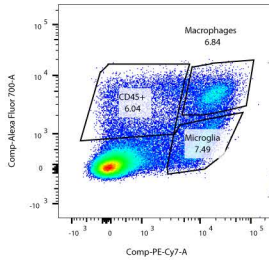
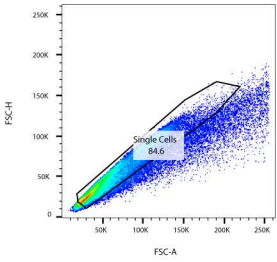
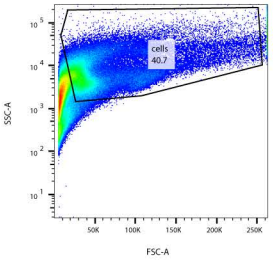
wild type naive brain



OPN^{-/-} naive brain



wild type GL261 tumor



OPN^{-/-} GL261 tumor

